PCCP

Accepted Manuscript

ROYAL SOCIETY OF CHEMISTRY

www.rsc.org/pccp

Physical Chemistry Chemical Physics RSCPublishing

ARTICLE

Cite this: DOI: 10.1039/x0xx00000x

Received 00th January 2012,
Accepted 00th January 2012

DOI: 10.1039/x0xx00000x

www.rsc.org/

The Effect of Oxidative Stress on Bursopentin Peptide Structure: A Theoretical Study

A. T. Lam,[a] E. P. Faragó,[b] M. C. Owen,[a,b] B. Fiser,[b] B. Jójárt,[b] S. J. K. Jensen,[c] I. G. Csizmadia[a,b] and B. Viskolcz[b]

Bursopentin (BP5, H-Cys[1]-Lys[2]-Arg[3]-Val[4]-Tyr[5]-OH), is found in the *bursa fabricius* of the chicken, is a pentapeptide that protects the organism from oxidative stress by reducing the intracellular generation of reactive oxygen species. Hydrogen abstraction, a common oxidative reaction occurring in proteins, often results in the formation of D amino acid residues. To study the effect of this phenomenon on the structure of bursopentin, each of its residues were converted from the L configuration to the D configuration, and the structure of these peptide epimers were compared to that of the wild-type bursopentin. The conformations, secondary structures, compactness and hydrogen bonding of bursopentin was compared to its epimers using molecular dynamics simulations and first principles quantum chemical computations. It was discovered that the repulsion between the side chains of Lys[2] and Arg[3] influenced the conformation of the peptide regardless of the configuration of these residues. Epimerisation of the Val[4] and Tyr[5] caused a reduction in the compactness of bursopentin. In all cases, the occurrence of a turn structure was relatively high, especially when Arg[3] was in the D configuration. Thermodynamic analysis of the epimerisation process showed that the formation of D amino acid residues in favourable.

Introduction

Converging evidence suggests that oxidative stress plays a role in a number of pathophysiological diseases such as Parkinson's disease (PD), Alzheimer's disease (AD), and atherosclerosis, just to mention a few of the more than 50 examples.[1-3] The mechanisms leading to cellular oxidative stress has been shown to result from the overproduction of reactive oxygen species (ROS), which are chemically reactive oxygen compounds that includes non radicals (i.e. H_2O_2) and free radicals (i.e. OH, O_2^-, CO_2 and NO). In turn, ROS can interact with different molecules, to initiate a cascade of events that can lead to cell death.[4] For example, protein oxidation is a result of hydrogen abstraction by hydroxyl radicals.[5] Under normal conditions, ROS are generated by the electron transport chain of the mitochondria and chloroplast and are reduced by the cell's antioxidant capacity.[5] When the antioxidant capacity can no longer reduce ROS they can accumulate in the cell. This can involve the oxidation of the side chain of amino acid residues, as well as the oxidation of the protein backbone, which can result in a) protein fragmentation b) a change from the L-configuration to the D-configuration c) protein aggregation and d) protein misfolding.[6] These four cases caused by an altered protein structure have been observed in a neurodegenerative disease such as Alzheimer's disease, which is generally found in the elderly.[7]

It was once thought that all living organisms are composed of only L-amino acids and that the enantiomers of L-amino acids were eliminated during the origin of life.[8] The discovery of D-aspartic acids (D-Asp) in various human tissues such brain, teeth skin, and lung of the elderly suggests that oxidative stress related to ageing is a main factor in the production of D amino acids. Such configuration change can result in the accumulation of the D -amino acids in the protein, which can alter the higher-order structure of the protein and decrease the original protein concentration.[9-12] Moreover, the accumulation of D-amino acids in the brain is affiliated with Alzheimer's disease.[11] This

observation strongly suggests that there is a direct correlation between D -amino acids, oxidative stress, and ageing. The Bursopentin (BP5, H-Cys[1]-Lys[2]-Arg[3]-Val[4]-Tyr[5]-OH), is a pentapeptide that is found in the bursa of Fabricius (BF) of a chicken immune system, and has been shown to protect living organisms from oxidative stress by reducing the intracellular generation of ROS.[14] Moreover, bursopentin contains a thiol functional group and can exert immunomodulator effects on B and T lymphocytes.[15] Reactive oxygen species (ROS) can act as second messengers to regulate transduction pathways that control gene expression and the modification of proteins.[16-18] In the presence of ROS, protein kinase (PKC) and mitogen-activated protein kinase (MAPK) are activated, thus inducing B-lymphocyte proliferation.[15] Bursopentin is an antioxidant and can function as an scavenger to prevent ROS from damaging DNA and RNA, and the oxidation of amino acid residues in proteins.[15] It has been shown that homocysteine (Hcy) can generate OH and O_2^- radicals through auto-oxidation and induced β-lymphocyte proliferation.[19] This suggests that the cysteine in BP5, is a possible cause in promoting β-lymphocytes proliferation as cysteine exhibits similar chemical properties to homocysteine through its sulphhydryl (-SH) group.[20,21] In turn, BP5 has a suppressive effect on the amount of oxidative stress observed in living cells.[14] Although, BP5 has the capability of reducing oxidative stress for different protein, BP5 can also be oxidized.

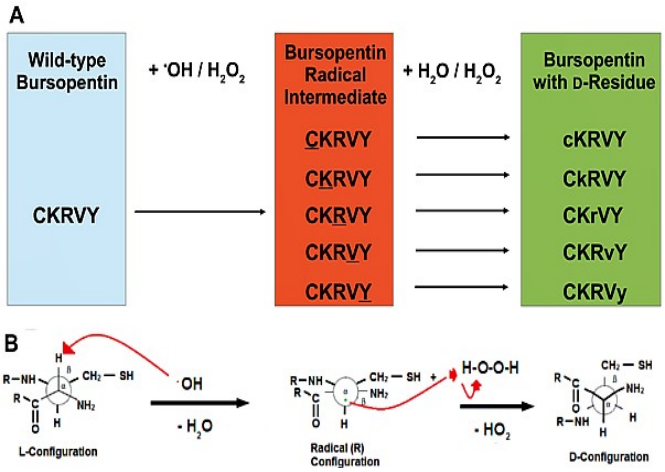

Scheme 1: General scheme describing the formation of radical intermediates and D-amino acid residues of bursopentin. The underlined residue contains the respective C_α-centered peptide radical, whereas the lower cased letter indicates the position of the D-amino acid residue **(A)**. The Newton Projection of the reaction mechanisms of CKRVY conformer at Cys[1] (**B**).

The oxidative attack on the polypeptide backbone of a protein is initiated by an abstraction of an α-hydrogen atom from an amino acid residue by the highly reactive hydroxyl radical to form an α-carbon radical.[22] The hydroxyl radical can be generated by the radiolysis of water or by a metal-catalyst cleavage of hydrogen peroxide.[8] H_2O_2 can restore the H atom by forming an unstable eclipsed transitional state, and the configuration of the peptide will transform from L to D, with a lowered activation barrier as shown in **Scheme 1**.

The formation of the D-configuration at each residue will alter the ϕ and ψ angles of the α-carbon, generating different secondary structures. Shown in **Figure 1,** the ideal angles, ϕ and ψ, are -60° and 60°, γ_L. The formation of residues in the D-generation of D-amino acids is formed by the oxidation of peptides, such as glutathione and bursopentin.[13] configuration may have ϕ and ψ angles that deviate from this value. Using **Figure 1,** one can classify the folding patterns of BP5 on the basis of the folding pattern of the model peptide residues.

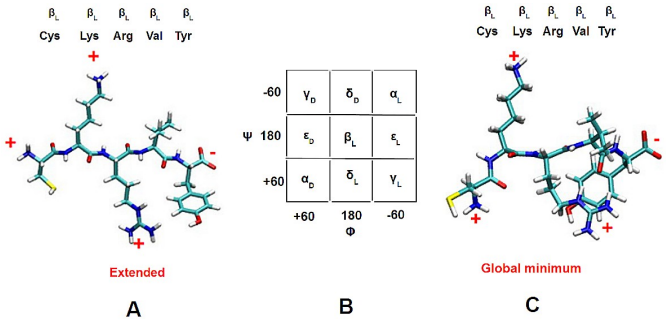

Figure 1. The structure of bursopentin in the extended conformation optimized at the B3LYP/6-31G(d) level of theory (A). The expected conformers of a peptide residue shown in Ramachandran space (B). global minimum bursopentin conformation computed at the B3LYP/6-31G(d) level of theory (C).

In this work, we provide a systematic and comparative analysis of the bursopentin structure both before and after the radical-initiated epimerisation using Molecular Dynamics and density functional theory (DFT). To the best of our knowledge, there have been no structural studies on bursopentin to date, neither by experiment nor computational means. Our work is the first to combine Molecular Dynamics (MD) and DFT to study the thermodynamics of the epimerisation of the C_α of each bursopentin residue and compare the structure of each respective peptide epimer to the structure of the wild-type bursopentin. Secondary structures, radius of gyration and hydrogen bonding of each peptide, and its affect on conformation and peptide activity is discussed.

Materials and Methods

The wild-type Bursopeptin (CKRVY) was constructed using the tleap module of the AmberTools 1.5 program package.[23] The chirality of each amino acid residue was manually changed from the L configuration to the D configuration to produce five epimers, cKRVY, CkRVY, CKrVY, CKRvY and CKRVy, where the residue in the D-configuration is shown in a lower-cased letter. The 3D structures of the pentapeptides were visually inspected in Visual Model Dynamics 1.9.[24]

The extended conformation of each of the peptides was optimized by the steepest descent (500 steps) and conjugated gradient method in a consecutive manner, which provided the initial structures for the simulated annealing (SA) protocol.[25] SA calculations were carried out with the sander module implemented in AMBER9.[26] The ff99SBildn force field, and the Generalized Born implicit solvent model were applied in each simulated annealing run.[27,28] The minimized structure was heated from 300 K to 1000 K over 1000 fs. At the maximum temperature, the structure was equilibrated for a duration of 4000 fs before being cooled to 500 K over 1000 fs, from 500 K to 200 K over 2000 fs and from 200 K to 50 K over 7000 fs. This simulated annealing protocol was repeated 2000 times to generate 2000 conformers for each peptide configuration. The

Ptraj program was utilized to perform structural analysis on the each peptide configuration. Hydrogen bonds were assigned when the distance between the heavy atoms of the donor (D) and acceptor (A) atoms is less than 3.5 Å and the angle A···H-D is greater than 100°. The Define Secondary Structure of Proteins (DSSP) algorithm, as implemented in the AmberTools 1.5 program package, was used to assign the secondary structural elements to each peptide residue[29] and the radius of gyration of peptide (Rgyr) was calculated according the following equation:

$$R_{gyr} = (\sum^{n}_{i=1} m_i (x_i - x)^2 / \sum^{n}_{i=1} m_i)^{½} \qquad (1)$$

In order to characterize the backbone conformation density, Ramachandran maps for 2nd, 3rd, 4th amino acid and pseudo Ramachandran maps for 1st and 5th amino acid were constructed. The percentage distributions of the structure are displayed on density maps where the length of each subspace was 10°. A structural analysis of the backbone was performed on each configuration (extended, global minimum, and rmsd) by taking the distance (Å) from the N-terminus to C-terminus of bursopentin.

Two conformers of each peptide were subsequently studied using density function theory (DFT). The first is the one with the lowest energy, and the second is the conformer with the structure that is most similar to that of the wild-type bursopentin conformer of lowest energy (RMSD). The RMSD conformer enabled the thermodynamics of the epimerisation to be quantified without any of the associated conformational changes. The geometry of these structures were optimized by density functional theory B3LYP method combined with 6-31G(d) basis set. All minimized structure was verified by harmonic vibrational analysis. To mimic the real molecular environment, the SMD implicit water model were applied to all calculations.[30] The changes in energy ΔE^o and the thermodynamic parameters ΔG^o, ΔH^o, and ΔS^o, for the epimerisation of the C_α of each residue was also computed at the B3LYP/6-31G(d) and B3LYP/6-311++G(d,p) levels of theory using electronic energies and unscaled frequencies. All DFT computation was carried out by Gaussian09 program package.[29]

Results and Discussion

Conformational Analysis by Molecular Dynamics Methods

The Effect of Oxidation on Radius of Gyration

The radius of gyration was used to compare the compactness of the wild-type BP5 to those of the epimerised peptide enantiomers. As shown in Figure 2, the wild type configuration (CKRVY) has two maxima distribution values. Therein shows that 21.8% of the structures had a radius of gyration of 5.75 Å, whereas 19.1% of the structures had a radius of gyration of 6.25 Å. The cKRVY, CkRVY and CKrVY have a similar radius of gyration distribution as the wild-type bursopentin because of the positive charges at each residue, as shown in **Figure 1**. The CKrVY peptide had the most compact structure, with both distribution peaks shifted to lower radius of gyration values than those observed in the wild-type. The CKrVY peptide had a lower maximum peak of ~18% of structures with a radius of gyration of 5.5 Å at its first peak and its second peak coincides with the wild-type bursopentin. This shows that the CKrVY has the most compact structure.

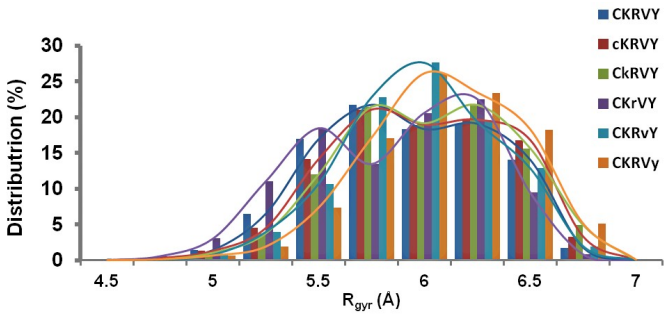

Figure 2. The distribution of the radius of gyration (Rgyr / Å) of the wild-type bursopentin and its epimers.

Therein shows that 21.8% of the structures had a radius of gyration of 5.75 Å, whereas 19.1% of the structures had a radius of gyration of 6.25 Å. The cKRVY, CkRVY and CKrVY have a similar radius of gyration distribution as the wild-type bursopentin because of the positive charges at each residue, as shown in Figure 1. The CKrVY peptide had the most compact structure, with both distribution peaks shifted to lower radius of gyration values than those observed in the wild-type. The CKrVY peptide had a lower maximum peak of ~18% of structures with a radius of gyration of 5.5 Å at its first peak and its second peak coincides with the wild-type bursopentin. This shows that the CKrVY has the most compact structure.

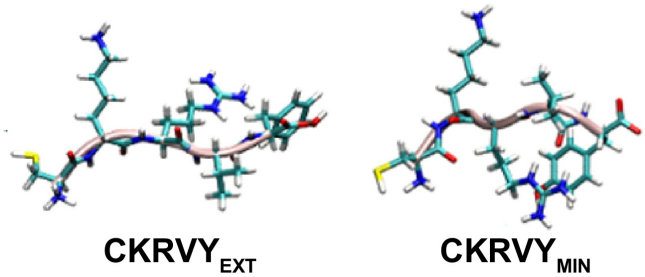

Figure 3. Representative conformations of wild type bursopentin in the extended and global minimum conformations.

The effect of the positive charge on the N-terminal amine and side chain of Lys[2] and Arg[3], creates repulsive interactions with each other. With the modification of the chirality of each residue, the direction of the positive and negative side chain with respect to the peptide backbone changed. This change could influence the electrostatic interactions which dictate the compactness of the bursopentin peptide. A more detailed analysis of the hydrogen bonding in bursopentin follows. Moreover, the CKRvY and CKRVy epimers deviated from the wild-type CKRVY since the curves for these structures contained a single peaks shown in **Figure 2**. At these configurations the molecule is less compact.

Secondary Structure Analysis of BP5 Epimers

The 3_{10} helix, α-helix, π-helix, β-pleated sheets (parallel and anti-parallel), and turn secondary structures of 2000 conformations of each peptide were analyzed using the DSSP algorithm (**Table S1**). The wild-type, CkRVY, CKrVY and CKRvY epimers have turn secondary structures that did not appear in the cKRVY and CKRVy epimers of bursopentin. The

global minimum and extended bursopentin structures are shown in **Figure 3**. Excluding the CkRVY configuration, the other peptides with D-configurations have both 3_{10} helical and turn secondary structures, as shown in **Figure 4**. The turn secondary structure element was present in each of the peptide enantiomers in the highest quantity.

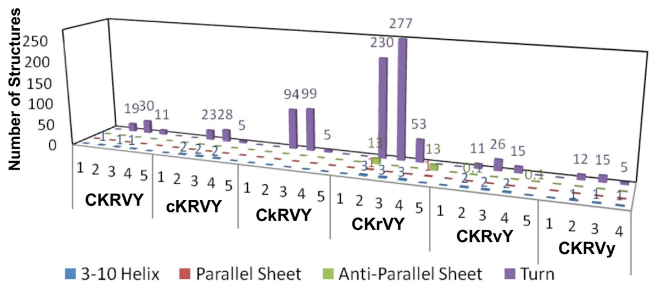

Figure 4: Secondary structure of wild type BP5 in comparison to its D-conformers in 2000 structures, where 1 to 5 represents the position of the residue.

This could be due to the length of the pentapeptide, which is favourable for the formation of turns but disfavours the formation of helices, which generally requires more residues to be stable. The stability of the turn structure may be enhanced due to the charge of the residues. The apparent attraction between the positively charged side chains of Lys^2 and Arg^3 and the negatively charged carboxyl terminus could be the reason for the high number of turn structures. A subsequent density analysis of this structure could confirm the nature of this interaction. The conversion to the D-configuration changes the direction of the side-chain from an upward to a downward (or vice versa) with respect to the peptide backbone. This change increased the number of turn structures in both the CkRVY and CKrVY peptides, which suggests that the distance between the charged entities of these groups was favourable for the formation of turns when the configurations changed from L to D.

The β-pleated sheet was observed in the CKrVY and CKRvY configurations. The CKrVY peptide had parallel and anti-parallel sheet at the 2nd and 5th position of CkrVY, respectively. At the CKRvY conformer only the anti-parallel sheet was present in residue Lys^2 and Tyr^5 (**Figure 5**).

Intramolecular Hydrogen Bonds

The 3_{10} helix and turn secondary structures are generally stabilized by intramolecular hydrogen bonds, however, these hydrogen bonds can also stabilize different conformational states. For instance, the stability of the global minimum CKRvY conformation is mainly due to the hydrogen bond between Tyr^5 and Arg^3. The intramolecular hydrogen bonds in wild-type bursopentin and its epimers are summarized in **Table 1**. The most frequently occurring hydrogen bonds in bursopentin and its epimers were between the side chain of amino acid residues and the peptide backbone. A hydrogen bond between the backbone of Lys^2 and the side chain of Arg^3 side chain was present in all of the peptides (**Figure 6**). Backbone-backbone hydrogen bonds were observed between Cys^1 and Arg^3 and between Lys^2 and Val^4, whereas side chain-side chain hydrogen bond was found between the Arg^3 and Tyr^5 residues. Among the peptides containing D-amino acids, the minimum number of hydrogen bonds was five. Hydrogen bonds interactions were observed between the five residues of BP5 due to the close proximity of the residues and the interaction

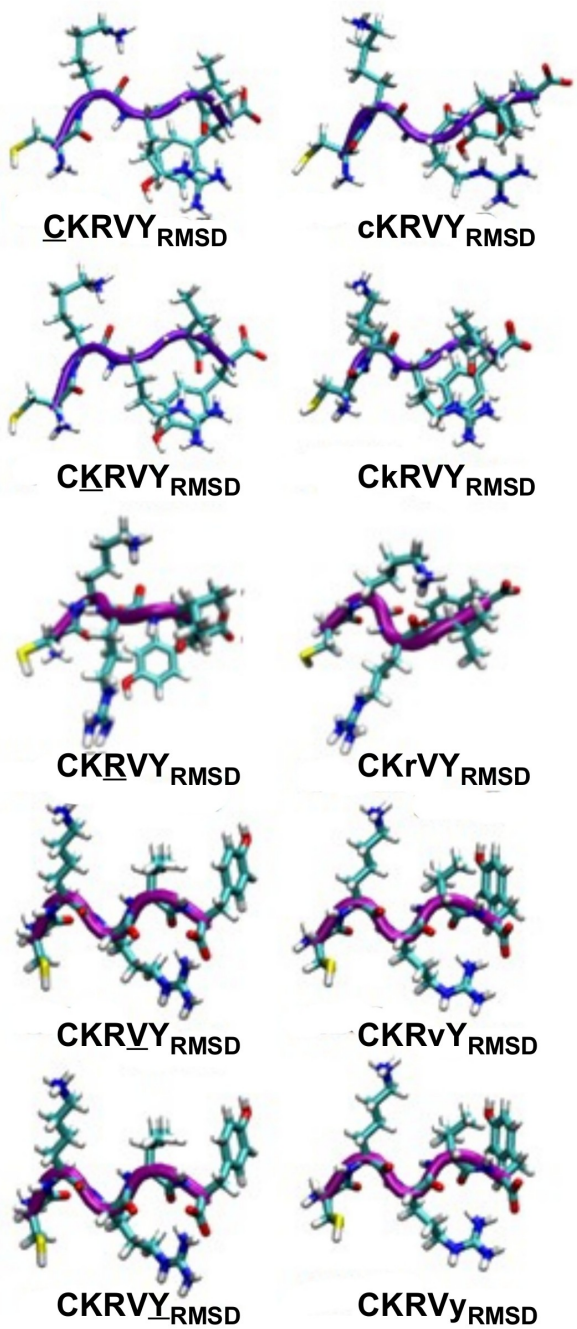

Figure 5. Representative conformations of the radicals and D-amino acids at each residue at RMSD.

between the side chains. For instance, Arginine and Lysine are basic amino acids containing nitrogen in their side chain and tyrosine containing a hydroxyl group. The oxygen and nitrogen in these residues can interact with the side chain and backbones to form the hydrogen bonds **(Figure 6)**.

Table 1. H bond interaction between the residue in BP5 above 5% occupied where (NF) represents less than 5% occupied.

Hydrogen Bonding Atoms	Peptide					
	CKRVY	cKRVYD	CkRVY	CKrVY	CKRvY	CKRVy
Cys^{1}_{BB} - Arg^{3}_{BB}	NF	NF	9.8	NF	NF	NF
Lys^{2}_{BB} - Val^{4}_{BB}	NF	5.2	NF	5.4	5.2	NF
Cys^{1}_{BB} - Arg^{3}_{SC}	6.2	6.0	NF	NF	6.5	5.65
Lys^{2}_{BB} - Arg^{3}_{SC}	8.3	7.2	8.8	14.8	14.9	7.30
Arg^{3}_{BB} - Lys^{2}_{SC}	8.0	9.4	NF	NF	11.3	10.05
Val^{4}_{BB} - Lys^{2}_{SC}	NF	NF	NF	NF	6.0	NF
Val^{4}_{BB} - Arg^{3}_{SC}	9.7	9.9	13.4	9.7	NF	21.6
Tyr^{5}_{BB} - Arg^{3}_{SC}	23.4	21.4	24.7	5.3	NF	62.4
Tyr^{5}_{SC} - Arg^{3}_{SC}	17.5	17.1	17.0	8.9	NF	NF

The quantitative amount of hydrogen bonds varied in each epimer. The most frequently observed hydrogen bonds are between the backbone of Lys^{2} and the side chain of Arg^{3}, the backbone of Val^{4} and the side chain of Arg^{3} and the backbone of Tyr^{5} and the side chain of Arg^{3}.

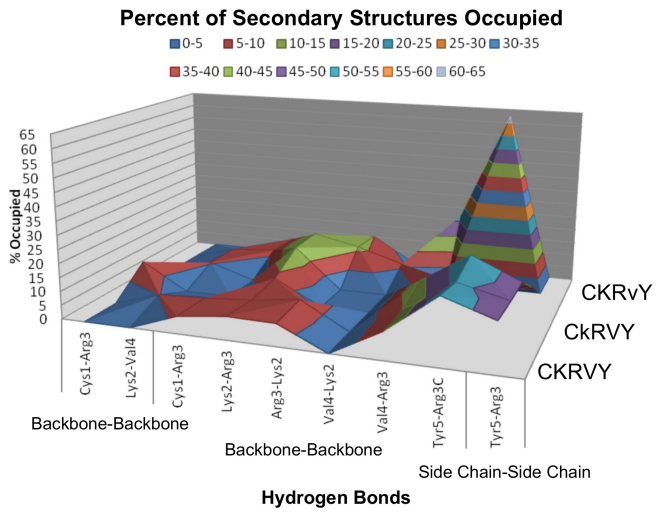

Figure 6. Hydrogen bond interaction between the residues in bursopentin.

The last hydrogen bond was observed most frequently (62.4% of the time) in the CKRVy peptide, which has Tyr^{5} in the D-configuration. The side chains are in close proximity to form hydrogen bonds, so this interaction can be found in almost every peptide epimer except in CKRvY, which does not show any hydrogen bonding between these atoms. This means that the change in chirality prevented hydrogen bonds from forming between the 3rd and 5th residues.

The Arg^{3} residue most frequently forms hydrogen bonds. The guanidinium side chain of this residue forms hydrogen bonds with the backbone of Lys^{2}. This interaction occurs most frequently in CKrVY (14.8 %) and CKRvY (14.9 %), both of which can be attributed to the D-configuration of the residue (**Figure 6**). The configuration change in the first and last residues reduced the formation of hydrogen bonds in cKRVY 7.2%, in CKRVy 7.3% compared to the wild-type peptide (8.3%). If the D-amino acid residue in the second position the hydrogen bond is almost same as in the case of the wild type bursopentin, so this configuration change does not influence the conformation significantly. The presence of this hydrogen bond in almost every peptide epimer demonstrates its significance.

Compared to the wild-type bursopentin, the cKRVY and CkRVY epimers have more hydrogen bonds due to the changes in configuration, steric changes and electrostatic interactions. The hydrogen bonding in these epimers are similar to those in the wild-type in many cases; for instance, four of the six hydrogen bonds in cKRVY, CkRVY and CKrVY are the same ones that are present in the wild-type peptide. The largest difference is shown in CKRvY because the change in configuration in the 4th position reduces the ability of Tyr^{5} to form hydrogen bonds, which reduces the number of hydrogen bonds in CKRvY.

The hydrogen bonding criteria used in this study (A---H-D > 100°) applies for traditional hydrogen bonds, where the the donating an accepting atoms are electronegative atoms such as O and N, as proposed by Pauli.[31] The use of these criteria instead of those of Pimental and McClelland[32], which do not restrict the atom types, excludes the contributions of weakly polar interactions involving hydrogen atoms that may also influence the peptide structure. Though not discussed explicitly, weakly polar interactions do influence peptide structures and this influence dictates their relative population of the 2000 conformers studied in this work. The omission of weakly polar interactions from the analysis limits the number hydrogen bonding interactions determined in this work. Subsequent analysis could include some form of density analysis, such as the Atoms in Molecules approach of Bader[33], which could characterize the interactions of some of the more biologically relevant conformers identified in this work.

B) Epimerization mechanism by *ab initio* methods

Structural Comparison of BP5 Bond Lengths

As expected, the C_{α}-C_{β} bond length in the D-configuration of each respective residue has approximately the same C_{α}-C_{β} bond length as found in the wild-type, and this was shown in previous studies[34,35] and demonstrated in the extended, global minimum and RMSD structures (**Table S2**). The peptide radicals had a C_{α}-C_{β} bond length that was 0.06 Å shorter than that at the respective residue in the wild-type peptide. The removal of the H_{α} from the peptide structure at each residue reduced the C_{α}-C_{β} bond length to accommodate for the loss of hydrogen. In turn C_{α}-C_{β} bonds are stronger in the peptide radicals. This tendency is also observed in the C_{α}-C bond and N-C_{α} bonds since an electron in C_{α} is missing its electron pair. The bond shortening was not observed in the C=O bond, N-H bond, the "n-1" amide bond nor in the "n+1" bond (β bonds). These bonds lengths are larger by 0.03 Å in the radical form at each residue and are thus weakened. It is possible that the change in bond length could be due to electron delocalisation, which enables the unpaired C_{α} electron to 'push' the electron

pairs on the N and O atoms further away from the radical centre.[31] The effect of the H_α abstraction can also be found in the β- and γ-bonds which is the same as in the α-bonds, but it is lower in magnitude because of the larger distance from the C_α.

Structural Analysis of the Peptide Backbone

The length (Å) of the backbone was measured from N-terminus to the C-terminus of bursopentin and each peptide epimer. In the extended conformation, the backbone (Å) of the wild-type bursopentin, the bursopentin radicals, and bursopentin epimers differ by approximately 1.5 Å. When Cys^1 or Lys^2 contains a C_α-centered radical or D amino acid residue the peptide's backbone length was greater than in the wild-type peptide. However, when the Arg^3, Val^4 or Tyr^5 residues are modified the length of the peptide is larger than the wild-type bursopentin. At the 1st and 2nd residue, the length of the backbone of the stereoisomer and radicals is approximately similar to the CKRVY configuration (**Table S2**). Only at the CkRVY configuration, a formation of hydrogen bond is present between the backbone of Cys^1 and Lys^3. The formation of such hydrogen bond inhibited the formation of a turn secondary structure. CkRVY lacked hydrogen bonds, less than 5% occupied, between the backbone of Lys^2 and Val^4 and between the backbone of Lys^2 and Arg^3 that appeared in other conformers. These hydrogen bonds cause the structure of the peptide to become more extended. Compared to the wild type, the percentages of the hydrogen bond in the D-conformers are slightly equivalent. This demonstrated the shape and length of backbones are quite similar to each other. The lowest hydrogen bonding values of **Table S4** belong to the CKrVY and the CKRVY structures. Interestingly, these structures have a relatively high number of turns despite the fact that they do not contain a large number of hydrogen bonds (**Table 1**). The significance of the hydrogen bonds decreases in the view of the secondary structure because of the repulsion between Lys^2 and Arg^3 which is more important than in other cases. The positive charge between the 2nd and 3rd residues causes steric hindrance pushing the residue further apart, thus, decreasing the ability hydrogen bond formation.

At the RMSD structures, the tendencies are similar to the extended form. The shortest backbone length of BP5 (Å) was the radical formation. The D-configurations are more compacted than the wild type.

The Effect of Oxidation on the ϕ and ψ Dihedral Angles

When the ϕ and ψ angles of the residues in the D configuration are compared to the those of the respective residue in the wild-type BP5, it is evident that the two sets of angles remain largely unchanged **Table 2**. This suggests that the configuration of the residue does not cause changes to the conformation of the peptide when it is in the extended conformation. This is also the case in the global minimum conformations, which shows that the change in configuration does not alter the structure of the global minimum conformation. Due to the stability of the planar conformations, where ϕ and ψ are close to 180°, in the peptide radicals can cause the peptide to unfold when in the radical state, and to refold when in the L or D epimerisation did not cause a significant change to the structure of bursopentin.

Table 2. Conformational assignment for a segment (from amino acid (AA) residue 2 to 4) of Bursopentin wild type extended conformer and D-configuration.

Parameter	Animo Acid Residue					
	L-Lys^2	L-Arg^3	L-Val^4	D-Lys^2	D-Arg^3	D-Val^4
ϕ / degree	-151.0	-153.0	-136.3	153.6	131.4	62.74
ψ /degree	-146.5	150.0	152.7	-140.7	-80.2	-144.25
Secondary Structure	β_I	β_I	β_I	β_I	δ_D	ε_D

The Effect of Epimerisation on Secondary Structure

The change in configuration caused the secondary structure of the epimerized peptides deviate from the secondary structure of wild type bursopentin peptide. The secondary structure of the wild type bursopentin contains a turn at the Lys^2, Arg^3 and Val^4 residues. Based on the Ramachandran maps these can be identified as various types of β-turns, because the typical ranges of φ and ψ dihedral angles are characterized. Converting the configuration of the Cys^1, Lys^2, Arg^3 and Val^4 residues from L to D causes the turn structure to be preferred. The structure of the CKRVy and cKRVY are the most similar to the wild type since epimerisation at these residues induced fewer turns. The structure of the CkrVY epimer deviated the most from that of the wild-type due to the numerous turns that this epimer formed.

Thermodynamic Properties of BP5

The change in enthalpy for the formation of each of the D peptide epimers in the extended conformation are endothermic except the CKRvY, whereas the change in enthalpy for these reactions in the global minimum conformation are endothermic also except CKRVy configuration when computed with the 6-31G(d) basis set. (**Table 3**). The change in enthalpy between the extended and global minimum of each conformers varied, **Table 3**, increasing tendency was observed from cKRVY to CKRVy configuration. In entropy the CKRVy peptide has a high change within its system at 61.1 J mol^{-1} K^{-1}. This may be due to the high percent (62.4%) of hydrogen bonding that occurred between Arg^3 and Tyr^5 in the structures. The relative free-energy is positive in almost in every case and shows decreasing tendency which means the conversion to the D-configuration is an energetically non-favourable process but getting on the 5th residue this process in extended form is becoming energetically more prosperous. In the case of CKRVy the formation of D peptide epimer is the most favourable because the hydrogen bond between Arg^3 and Tyr^5 makes much more stable the structure. The difference in the relative free energy between the extended and global minimum is very various, the lowest value belongs to the CKRVy structure. This is the only one case where the global minimum has lower relative free-energy than the extended configuration due to the formation of the secondary structure and the stabilizing effect of the hydrogen bonds.

Thermodynamics of Epimerisation Reaction

The energetic of radical formation and epimerisation is summarized in **Figure 7**. The enthalpy values are very different for each of the peptides in the extended conformation. In general the formation of the radicals is in all case exothermic.

The most favourable process is the formation of CKRVY which belongs to the highest entropy value in extended conformation.

Table 3. The change in enthalpy (ΔH^o), free energy (ΔG^o) and entropy (ΔS^o) in the reactions between OH and bursopentin at the C_α of residue X computed at the B3LYP/6-311++G(d,p) level of theory, whereas the B3LYP/6-31G(d) values are shown in parenthesis.

Structure		Energetics of Epimerization Steps					
		To Form the Radical Intermediate			To Form the D-Configuration		
Res. Num.	Conf.	ΔH^o / kJ mol^{-1}	ΔG^o / kJ mol^{-1}	ΔS^o / J mol^{-1} K^{-1}	ΔH^o / kJ mol^{-1}	ΔG^o / kJ mol^{-1}	ΔS^o / J mol^{-1} K^{-1}
1	EXT	-90.7 (-89.0)	-92.2 (-90.4)	4.8 (4.8)	1.8 (8.8)	-2.4 (4.6)	44.9 (14.0)
	GM-RMSD	-78.7 (-81.7)	-75.2 (-78.2)	-14.6 (-15.0)	11.9 (10.5)	15.4 (14.0)	6.2 (-11.7)
2	EXT	-128.7 (-132.1)	-132.0 (-135.5)	11.3 (11.3)	-1.9 (3.2)	-1.0 (4.0)	-2.8 (-2.8)
	GM-RMSD	-98.5 (-106.9)	-86.4 (-97.9)	-43.2 (-43.2)	4.1 (9.6)	4.3 (9.7)	-0.6 (-0.6)
3	EXT	-118.0 (-121.4)	-119.4 (-122.8)	4.7 (4.7)	-1.3 (6.0)	-8.1 (-0.8)	22.7 (22.7)
	GM-RMSD	-87.9 (-96.2)	-82.7 (-91.0)	-20.4 (-20.4)	8.1 (16.9)	13.0 (21.8)	-16.4 (-16.4)
4	EXT	-103.0 (-109.2)	-102.6 (-108.8)	-1.4 (-1.4)	-12.2 (-0.3)	-16.9 (-4.4)	15.7 (15.7)
	GM-RMSD	-75.6 (-78.0)	-76.5 (-78.9)	0.4 (0.4)	17.1 (16.3)	17.7 (16.9)	-2.2 (-2.2)
5	EXT	-120.7 (-122.9)	-120.9 (-123.1)	0.5 (0.5)	-4.21 (7.9)	-17.4 (-5.29)	44.1 (44.1)
	GM-RMSD	-98.1 (-114.1)	-88.1 (-104.1)	-36.4 (-36.4)	-8.3 (-15.8)	-3.2 (-10.7)	-17.0 (-17.0)

In the global minimum conformation the CKRVY has the lowest value in the enthalpy (-114.1 J mol^{-1} K^{-1}) and relative free energy (-104.1 J mol^{-1} K^{-1}). The highest enthalpy (-89.0 J mol^{-1} K^{-1}) belongs to the CKRVY conformation. The enthalpy and relative free-energy of CKRVY and CKRVY are very close, almost the same, maybe there is similar stabilizing effect in these two cases. The relative free-energy values for the radical formation are all negative since the hydrogen abstraction is a spontaneous process.

The ΔS^o for the radical formation increased in the CKRVYEXT, CKRVYEXT, CKRVYEXT peptides, whereas the entropy decreased in the remaining structures which indicated that radical formation generally increased the disorder of the peptide. Radical formation in these peptides destabilized the turn, bend and helical secondary structural elements.

To form the D-configuration of the respective bursopentin residues when the peptide is in the extended conformation, the ΔH^o values must be close to zero. This signifies that the energy of these structures are close to equilibrium. The ΔG^o values for the hydrogen addition to form the D residue are positive in almost every case. Since the ΔS^o values are negative in many cases, which gain in structural order, the formation of D configurations can be generally considered to be a spontaneous process.

The ΔS^o for the radical formation increased in the $\underline{C}$KRVY$_{EXT}$, C$\underline{K}$RVY$_{EXT}$, CK$\underline{R}$VY$_{EXT}$ peptides, whereas the entropy decreased in the remaining structures which indicated that radical formation generally increased the disorder of the peptide. Radical formation in these peptides destabilized the turn, bend and helical secondary structural elements.

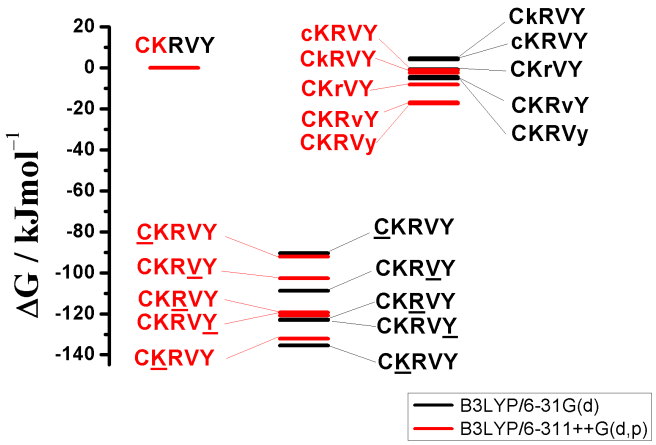

Figure 7. The relative Gibbs free energy of the radicals conformers in extended in comparison to wild type, as computed at the B3LYP/6-311++G(d,p) (red) and B3LYP/6-31G(d) (black) levels of theory. The radical formation is an energetically favourable process. The CKrVY conformer is more stable than CKRVY due to the turn structure, which is stabilized by the H-bond.

To form the D-configuration of the respective bursopentin residues when the peptide is in the extended conformation, the ΔH^o values must be close to zero. This signifies that the energy of these structures are close to equilibrium. The ΔG^o values for the hydrogen addition to form the D residue are positive in almost every case. Since the ΔS^o values are negative in many cases, which gain in structural order, the formation of D configurations can be generally considered to be a spontaneous process.

Conclusions

By conducting a conformational analysis on BP5 through molecular mechanics and molecular dynamics, we can conclude that the compactness, secondary structure, and hydrogen bonding within the peptide were manly influenced by side chain-side chain interactions. The compactness of the peptide was influenced by electrostatic interaction between the residues, the attractive interactions increased and the repulsive interactions decreased the compactness. Hence, the structures of cKRVY, CkRVY, and CKrVY configuration were similar to the wild-type Bursopentin structure. In turn, the structure of CKRvY and CKRVy differed from the wild-type Bursopentin since there was an attractive interaction between the side chains of Val^4 and Tyr^5. The percentage of turn secondary structure in each BP5 configurations was extremely high in relations to each parallel D-configuration. The CKrVY peptide has the highest degree of turn structure due to steric hindrance between Lys^2 and Arg^3, and two bulky groups (Arg^3 and Val^4.) Although, side chain-side chain interactions influence the compactness and percentage of various secondary structures, backbone-side chain hydrogen bonds were present in all D-configurations. The hydrogen bond between the backbone of Lys^2 and the side chain of Arg^3 was present in all the peptides.

Although the effect of oxidative stress on the structure of BP5 was examined in this study, the lack of change in the structure of the reduced and epimerised BP5 indicates that bursopentin can conserve its structure after epimerisation. This suggests

that the function of bursopentin could also be conserved as well as potential therapeutic uses to prevent the accumulation of modified proteins induced by ROS that are associated with a number of age-related pathologies such as Alzheimer's diseases (AD) and Parkinson's disease (PD). Therefore, BP5 may become a new anti-oxidative therapeutic approach to combat the accumulation of ROS and the induction of oxidative stress.

Acknowledgements

We thank László Müller and Máté Labádi for the administration of the computing systems used for this work. This work was supported by ''New functional material and their biological and environmental answers'' (project ID: TAMOP-4.2.2.A-11/1/KONV-2012-0047).

Notes and References

[a] Department of Chemistry, University of Toronto, 80 St. George St., Toronto, Ontario, Canada, M5S

[b] Drug Discovery Research Center, Department of Chemical Informatics, Faculty of Education, University of Szeged, Boldogasszony sgt 6, Szeged, Hungary-6725

[c] Department of Chemistry, Langelandsgade 140, University of Aarhus, DK-8000 Aarhus C, Denmark

Electronic Supplementary Information (ESI) available: Bond lengths and dihedral angles within residue 3 of bursopentin. See DOI: 10.1039/b000000x/

1. Barnham, K. J.; Masters, C. L.; Bush, A. I. *Nat. Rev. Drug Discov.* **2004**, *3*, 205-214.
2. Owen , M. C.; Szőri, M.; Csizmadia, I. G.; Viskolcz, B. *J. Phys. Chem. B* **2012**, *116*, 1143-1154.
3. Büeler, H. *Exp. Neurology* **2009**, *218*, 235-246.
4. Easton, C. *J. Chem. Rev*. **1997**, *97*, 53-82.
5. Stadtman, E. R. *Free Radic. Res.* **2006**, *40*, 1250-1258.
6. Berlett, B. R.; Stadtman E. R. *Biochem. J.* **1997**, *3241*, 1-18.
7. Gregersen, N.; Bolund, L.; Bross, P. *Mol. Biotechnol.* **2005**, *31*, 142-149.
8. Harris, E. D. *FASEB J.* **1992**, *6*, 2675-2683.
9. Shapira, R.; Chou, C. H. *Biochem. Biophys. Res. Commun.* **1987**, *146*, 1342-1349.
10. Masters, P. M. *Calcif. Tissue Int.* **1983**, *35*, 43-47.
11. Fujii, N. *Bio & Pharm.* **2005**, *28*, 1585-1589.
12. Shapiro, S. D.; Endicott, S. K.; Province, M. A.; Pierce, J. A.; Campbell, E. J. *J. Clin. Invest.* **1991**, *87*, 1828-1834.
13. Fiser, B.; Szőri, M.; Jójárt, B.; Izsák, R.; Csizmadia, I. G.; Viskolcz, B. *J. Phys. Chem*. **2011**, 115, 11269-11277.
14. Li, D. Y.; Xue, M. Y.; Geng, Z. R.; Chen, P. Y. *Cell.Physiol. Biochem.* **2011**, 29, 9-20.
15. Li, D. Y.; Geng, Z. R; Zhu, H. F.; Wang, C.; Miao, D. N.; Chen, P. Y. *Amino Acids,* **2011**, *40*, 505-515.
16. Burgoyne, J. R.; Mongue-Din, H.; Eaton, P.; Shah, A. M. *Circ. Res.* **2012**, *111*, 1091-1106.
17. Novotny, G. W.; Lundh, M.; Backe, M. B.; Christensen, D. P.; Hansen, J. B.; Dahllöf, M. S.; Pallesen, E. M.; Mandrup-Poulsen, T. *Arch. Biochem. Biophys.* **2012**, *528*, 171-184.
18. Davies, K. J. A. *J. Biol. Chem.* **1987**, *262*, 9895-9901.
19. Zhang, G. *Cardiovasc. Res.* **2001***, 52,* 328-336.
20. Toohey, J. I. *J. Supramol. Struct. Cell Biochem.* **1981**, *17*, 11-25.
21. Hamilos, D. L.; Zelarney, P.; Mascali, J. J. *Immunopharmacology* **1989**, *18*, 223-235.
22. Wolff, S. P.; Dean, R. T. *Biochem. J.* **1986**, *234*, 399-403.
23. Case, D. A.; Cheatham III, T. E.; Darden, T.; Gohlke, H.; Luo, R.; Merz Jr., K. M.; Onufriev, A.; Simmerling, C.; Wang, B.; Woods, R. J. *J. Comput. Chem.* **2005,** *26***,** 1668-1688.
24. Humphrey, W.; Dalke, A.; Schulten, K. *J. Mol. Graphics 14.1* **1996,** 33-38.
25. Leitgeb, B. *Chem. Biol. Drug Des.* **2005,** *79*, 313-325.
26. Case, D. A; et al. AMBER 11, **2010**, University of California, San Francisco.
27. Lindorff-Larsen, K.; Piana, S.; Palmo, K.; Maragakis, P.; Klepeis, J. L.; Dror, R. O.; Shaw, D. E. *Proteins* **2010,** *78,* 1950-1958.
28. Hawkins, G. D.; Cramer, C. J.; Truhlar, D. G. *Chem. Phys. Lett.* **1995,** *246*, 122-129.
29. Hanson, R. M; Kohler, D.; Braun, S. G. *Proteins* **2011**, *79*, 2172-2180.
30. Aleksandr, V. M.; Christopher, J. C.; Donald, G. *J. Phys. Chem. B* **2009**, *113,* 6378-6396.
31. Pauling, L. *The Nature of the Chemical Bond*, 3rd ed.; Cornell Univ. Press: Ithaca, NY, 1960 1960; Chapter 12.
32. Pimentel, G. C.; McClelland, A. L. *The Hydrogen Bond*; W. H. Freeman: San Francisco, CA, 1960.
33. Bader, R. F. W. *Chem. Rev.*, 1991, 91, 893–928
34. Owen, M. C.; Viskolcz, B.; Csizmadia, I. G. *J. Phys. Chem. B* **2011**, *115*, 8014-8023.
35. Owen, M. C.; Viskolcz, B.; Csizmadia, I. G. *J. Chem. Phys.* **2011**, *135*, 035101.